Desalination and Water Treatment
www.deswater.com

doi: 10.5004/dwt.2018.21870

104 (2018) 169–174
February

Adsorption of heavy metals on activated carbons and their respective lignocellulosic precursors: experimental and theoretical approach

Alejandra Alicia Peláez Cid[a,*], Ana María Herrera González[b], Martín Salazar Villanueva[a]

[a]*Facultad de Ingeniería BUAP, Edificio ING1, Ciudad Universitaria, CP 72570, Puebla, Puebla, Mexico, Tel. +52 222 2295500 Ext. 7610; emails: alejandra.pelaez@correo.buap.mx, alalpeci@hotmail.com (A.A. Peláez Cid), msalaz_77@hotmail.com (M. Salazar Villanueva)*
[b]*Instituto de Ciencias Básicas e Ingeniería UAEH, Ciudad del conocimiento, CP 42184, Mineral de la Reforma, Hidalgo, Mexico, email: mherrera@uaeh.edu.mx, anamhg_1@hotmail.com*

Received 25 August 2017; Accepted 30 December 2017

ABSTRACT

This work reports the application of lignocellulosic adsorbents and activated carbons prepared from vegetable residues in the removal of five heavy metals. The selected residues were: prickly pear peel, broccoli stem, white sapote seed, and agave fiber. The adsorption of heavy metals was studied individually, in mixture, and varying the pH of the aqueous solutions. For lead, individual adsorption rates of 3.07 and 6.67 mg/g (more than 97% removal) were reached using lignocellulosic adsorbents and activated carbons, respectively, at pH = 1. When found in mixture containing the five heavy metals, their individual adsorption rates decreased, but the global amount of metals adsorbed increased (9.98 mg/g). When pH = 2, the adsorption capacity of the activated carbons was increased twice. For the carbon produced with the agave fiber, it was 19.55 mg/g. This was the carbon with the largest adsorption capacity for heavy metals. The best lignocellulosic adsorbent to remove the heavy metals was that prepared from broccoli stem. Considering that carbonaceous materials contain layers of graphene in their structure, the interaction between metallic nanoparticles was modeled on a graphene surface using the software DMo13, and the order of adsorption of heavy metals on activated carbons nearly agreed with the adsorption energies predicted by the theoretical modeling.

Keywords: Vegetable residues; Lignocellulosic adsorbents; Activated carbons; Heavy metals adsorption; DFT calculations

1. Introduction

The excessive liberation of heavy metals into the environment caused by urban industrialization represents a major worldwide problem [1–3]. Activities such as mining, metallurgy, soldering, forging, photography, petrochemistry, production of iron, steel, and batteries for energy storage, as well as many others generate effluents with high contents of heavy metals [1–6]. Although metals such as Fe, Zn, Cu, and even Cr are essential to the human body, it has been proven that high concentrations of these are toxic and carcinogenic [6,7]. These can cause health issues ranging from mild to severe such as nausea, vomit, cramps, skin irritation, seizures, pulmonary fibrosis, damage in the central nervous system, kidneys, or liver, and even death [6,8]. Hence, their elimination from industrial effluents before they pollute receiving waters is necessary. The most common methods to eliminate heavy metals are chemical precipitation, ion exchange, coagulation–flocculation, membrane filtration, reverse osmosis, and adsorption [1–9]. The process of adsorption using activated carbons (AC) is the most versatile and widely used [10]. Because AC is a relatively expensive material [1], increasing attention has turned to the production of low-cost adsorbents from wastes such as *Pinus halepensis* [5] and Meranti wood sawdust [11], rice husk, fly ash [10], and chicken feathers [7], or AC prepared from walnut, hazelnut, almond, pistachio shell [2], apricot stone [2–4], and coffee residue [12]. Using wastes of vegetable origin to

* Corresponding author.

obtain lignocellulosic adsorbents (LA) [13] or AC to be used for the removal of heavy metals is an ever-developing alternative. The use of such residues has the following advantages: reduction and usage of solid wastes, ability to be transformed into AC with a high specific surface area as the result of the manipulation of the variables that control their development, ecological and economical cost reduction in the production of such carbons avoiding the use of wood, and no need to regenerate the adsorbents once they have been exhausted because of their low-cost production. The novelty of this work resides in the application of almost void-cost vegetable residues and low-cost AC in the removal of industrial pollutants which are highly harmful to the environment and to human beings such as heavy metals. The goals of this work were to reduce solid vegetable wastes and to prepare LA and AC for the adsorption of five toxic heavy metals commonly found in industrial wastewaters.

2. Materials and methods

The vegetable residues used to prepare the LA and AC were prickly pear peel, broccoli stem, white sapote seed, and agave fiber. In Mexico, all of them are generated in large amounts which guarantee their availability to produce the adsorbents [14,16,18]. For the preparation of the LA, the vegetable residues were only washed, dried, and grounded. The carbons were obtained by means of chemical activation with H_3PO_4 and carbonization at 673 K during 3 h. Preparation and characterization of both LA and AC have been reported in detail previously [14–18]. The adsorbents were used in granular forms with particle sizes ranging between 0.25 and 0.84 mm with the exception of FAgaNat and CarAgaQ which were fibrous adsorbents. Batch experiments were conducted to investigate the adsorption of metals on LA and AC. Because of the higher specific surface area of AC [18] compared with LA, the dose of carbons (5 g/dm^3) used during the processes of static adsorption at 303 K was half than that of LA (10 g/dm^3). The time of contact between the AC and the aqueous solutions containing heavy metals was 24 and 48 h for LA. The salt used to prepare the aqueous solutions for all metals was nitrate. All chemicals used were analytical grade (Merck, Germany). The studied heavy metals (Pb, Zn, Cu, Fe, and Cr) were selected because all of them are commonly found in wastewaters [1,2,6,9,10,16]. The initial concentration of metals in the aqueous solutions containing heavy metals was 30 mg/dm^3 both individually and in the mixture. The concentration of tested heavy metals was determined by means of atomic absorption spectrophotometry using a Perkin-Elmer atomic absorption spectrophotometer model 2380 with flame atomizer.

The calibration curves which were used to quantify the metals are shown in Table 1.

The amount of metal adsorbed (a) in mg/g was determined using Eq. (1):

$$a = \frac{V(C_i - C_f)}{m} \tag{1}$$

where V is the solution volume in dm^3, C_i and C_f are the initial and final concentrations in mg/dm^3, respectively, and m is the mass of adsorbent in g.

2.1. Functional groups and pH_{PZC}

The functional groups found in the LA and the AC were determined by means of infrared spectrophotometry with Fourier transform (FTIR) using a Spectrum One Perkin-Elmer spectrophotometer with attenuated total reflectance in the spectral interval between 4,000 and 650 cm^{-1}. The pH at the point of zero charge which quantifies the total charge of the surface was determined for LA and AC previously [14–18]. The functional groups found in the adsorbents and their point of zero charge (pH_{PZC}) are summarized in Table 2.

Table 2
Main functional groups present in the adsorbents prepared and point of zero charge

Adsorbent	Functional groups	pH_{PZC}	Reference
CarAgaQ	C=O, C=C aromatic, P–O–C, –PO_4	2.2	[16]
FAgaNat	O–H, C–H, C=O, N–H, C–O–C	4.6	[16]
CarTunaQ	O–H, C=O, N–H, C–O, P–O, P–O–C	2.1	[18]
Tuna	O–H, C–H, C=O, C=C aromatic, C–O–C	6.2	[14]
CarBrocQ	O–H, N–H, C=O, C–O, P–O–C, P–O	2.2	[18]
BrocNat	O–H, C–H, C=O, C=C aromatic, C–O–C	7.0	[15]
CarZapQ	O–H, C–H, N–H, C–O, P–O	2.3	[18]
EmbZap	O–H, C–H, N–H, C=O, C=C aromatic	5.9	[17]

Table 1
Information and analysis conditions of the studied heavy metals

Heavy metals	Salt	Electronegativity	λ (nm)	Calibration curves	R^2
Pb(II)	$Pb(NO_3)_2$	2.33	217	C = Abs/0.0236	0.9912
Zn(II)	$Zn(NO_3)_2$	1.65	214	C = Abs/0.2883	0.9979
Cu(II)	$Cu(NO_3)_2$	1.90	325	C = Abs/0.0653	0.9987
Fe(III)	$Fe(NO_3)_3$	1.83	248	C = Abs/0.0248	0.9977
Cr(III)	$Cr(NO_3)_3$	1.66	358	C = Abs/0.0053	0.9940

2.2. pH of the aqueous solutions

The pH of the aqueous phase is one of the most important factors that influence not only the dissociation of the functional active sites in the adsorbents, but also controls the speciation of metals. Because the pH plays a determining role [2–7,10–14], its effect during the adsorption of the heavy metals on AC was examined. The initial pH of the solutions was 1 and 2. This small interval in pH was chosen in order to avoid the precipitation of metallic salts and to establish similar conditions to those of the wastewater from industries that discard heavy metals.

2.3. Computational methodology

Considering that carbonaceous materials contain layers of graphene in their structure [13,19], the interaction between metallic nanoparticles on a nanosheet of graphene (NG) surface was modeled, and the results were compared with the experimental results obtained during the adsorption of metallic ions on the AC prepared from vegetable residues. In this study, total energy and electron properties were obtained by using density functional theory (DFT) [20], as implemented in the DMol3 software [21,22]. The generalized gradient approximation has been chosen to describe the exchange–correlation interaction with the parameterization proposed by Yang et al. [23]. A basis set composed of a double numerical basis (4s and 3d) with polarized function (4p) was selected, and for this study, an all-electron calculation has been considered. The convergence criterion of optimization was set to 1×10^{-5} eV/Å for the energy gradient and 5×10^{-4} Å^{-1} for the atomic displacements. The density of charge converged at 1×10^{-6}, which allowed a total energy convergence of 1×10^{-5} eV. In the generation of the numerical basis sets, a global orbital cutoff of 5.2 Å was used. All calculations were carried out without spin restrictions, which allowed to establish the lowest energy geometries. The condition of non-complex frequencies was established as the stability criterion for the studied systems. The electronic gaps were evaluated for the lowest energy structures from their corresponding energy differences between the Highest Occupied Molecular Orbital and Lowest Unoccupied Molecular Orbital. The NG with chemical composition $C_{54}H_{18}$ was used to simulate the periodicity of graphene and, in this way, to calculate the corresponding adsorption energy of metals on this geometry. The initial geometries were: lineal, equilateral triangle and regular tetrahedron for $N = 2$, 3, and 4, respectively (Fig. 1). The bonding zone is marked in Fig. 2.

The adsorption energy (E_{ads}) was calculated with the next general expression:

$$E_{ads} = (E_{NG-M_n}) - (E_{NG} + E_{M_n}) \quad (2)$$

where E_{NG-M_n}, E_{NG}, and E_{M_n} are the total energies associated to NG plus the metallic cluster (n = 2, 3, and 4), the individual nanosheets of graphene, and the metallic cluster (n = 2, 3, and 4), respectively.

3. Results and discussion

3.1. Individual adsorption of heavy metals

Fig. 3 shows the amount adsorbed and the removal percentage (above the bars) by the AC (Fig. 3(A)) and LA (Fig. 3(B)) when the metals were found individually at pH = 1. The adsorption order of heavy metals on AC (Fe > Pb > Cu > Cr > Zn) was different compared with LA (Pb > Cu > Fe > Cr > Zn). This occurs because of the different nature of both kinds of adsorbents. The order of adsorption of AC was: CarAgaQ > CarTunaQ > CarZapQ > CarBrocQ. The point of zero charge for all the carbons (2.1–2.3) indicates the acid character of their surface caused by the chemical activation with H_3PO_4, and this aids not only the adsorption caused by the porosity of the AC but also the chemical interaction with cationic species such as heavy metals by means of ion exchange. CarAgaQ was the only carbon which did not contain amine groups (Table 2) which are considered to have a basic character, thus eliminating the forces of repulsion with the metals and increasing the amount adsorbed on its surface. The order of adsorption of LA was: BrocNat and Tuna > EmbZap > FAgaNat. In the case of the LA, the retention of the metals is caused primarily by dipole–dipole forces with polar groups –OH, C=O, and C–O–C (Table 2), which are characteristic of lignocellulosic materials, with the metallic ions. In Fig. 3(A), it can be observed that the amount of metals adsorbed on the surface of the AC is almost twice as much as that adsorbed in the LA (Fig. 3(B)). In AC, the greater adsorption is attributed due to the presence of superficial

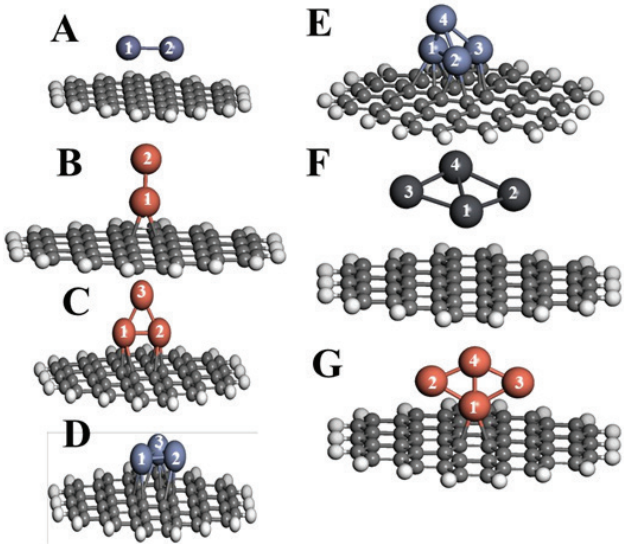

Fig. 1. Initial configuration: models (A), (D) and (E). Final configuration: models (B), (C), (F) and (G) for NG–Cu_2, NG–Cu_3, NG–Pb_4 and NG–Fe_4, respectively.

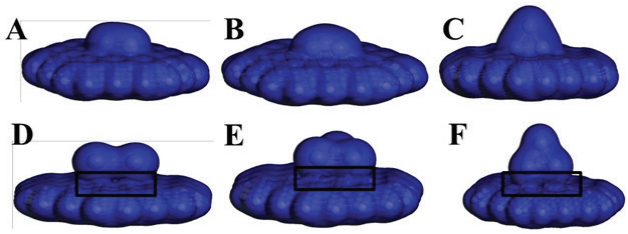

Fig. 2. Isosurfaces of electronic density at 0.017 Å^3 for the systems: (A) NG–Fe_2, (B) NG–Fe_3, (C) NG–Fe_4, (D) NG–Zn_2, (E) NG–Zn_3, and (F) NG–Zn_4.

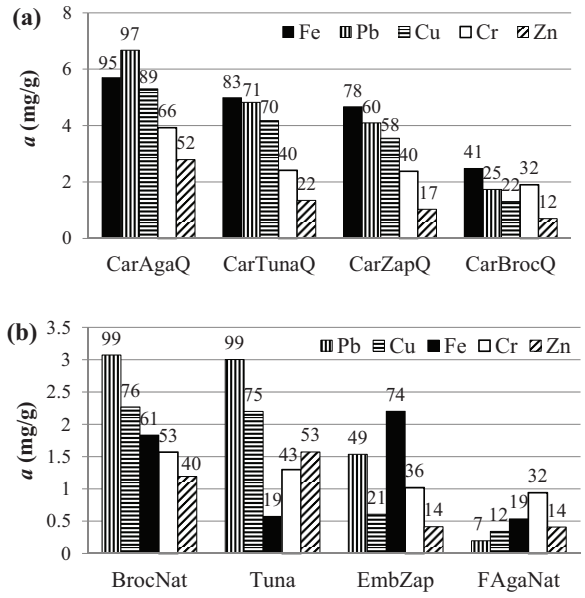

Fig. 3. Adsorbed amount and removal percentage of heavy metals present individually in aqueous solutions on the AC (A) and on the LA (B).

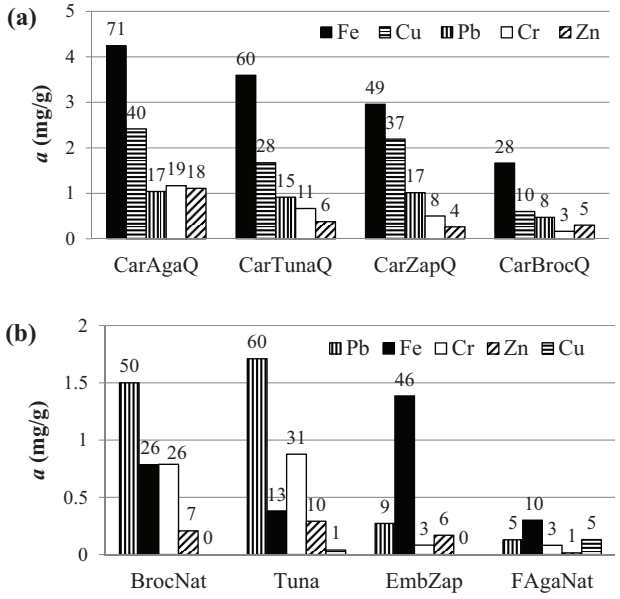

Fig. 4. Adsorbed amount and removal percentage of heavy metals present in mixture on the AC (A) and on the LA (B).

anionic groups, the strong anionic character of their surface, the porosity, and the high specific surface area of the carbons (1,025 $m^2/g < S_{BET} < 1,177\ m^2/g$) [18].

3.2. Adsorption of heavy metals in mixture

Fig. 4 shows the amount adsorbed by the AC and LA when the metals were found in a mixture at pH = 1. Now, the adsorption order of heavy metals on AC changed slightly: Fe > Cu > Pb > Cr > Zn. This indicates that the presence of other metallic ions modifies their interaction with the surface. The order of adsorption capacity of the AC and LA did not change, regardless of the metals being found alone or in a mixture. The AC with the largest adsorption capacity was CarAgaQ and the best of the LA was BrocNat and Tuna. Taking into consideration that Pb and Cr are some of the most dangerous and non-biodegradable persistent heavy metals because of their toxicity (lead may cause damage to the central nervous system, kidneys, liver, reproductive system, as well as to the functions and processes of the brain, and chrome can be the cause of severe health problems ranging from skin rashes to lung cancer [6]), the use of low-cost adsorbents such as the ones prepared in this work to fully or partially eliminate them is convenient.

Comparing Figs. 3 and 4, it can be observed that, when the metals were found in mixture, the individual adsorbed amounts decrease, but, globally, the adsorption capacity of the AC increases (Fig. 5(A)).

3.3. Improvement in adsorption of heavy metals in mixture at pH 2

The adsorption of heavy metals is critically linked to the pH. When the pH of the aqueous mixture is less acid, pH = 2 (Fig. 5(B)), the adsorption is promoted (it was almost double in all the carbons) because there is a smaller amount of protons competing for the anionic sites present in the AC.

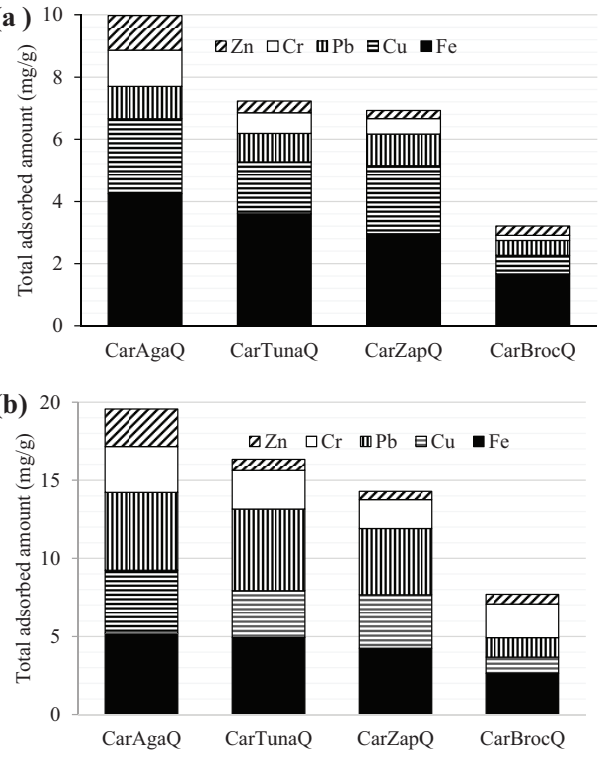

Fig. 5. Total adsorbed amount on the AC prepared at pH = 1 (A) and pH = 2 (B).

3.4. Computational results

The ground state was found for each of the systems considered in this study, for NG–M_n systems, where M = Fe, Cr, Cu, Pb, and Zn and n = 2, 3, and 4, the adsorption energy (E_{ads}) was established, and the values are shown in Table 3. Furthermore, bond distance ($D_{a–s}$) between metallic cluster

Table 3
DFT calculations using the software DMol3 for the corresponding systems

System	E_{ads} (eV)	D_{a-s} (Å)	Mulliken charges			
			Atom 1	Atom 2	Atom 3	Atom 4
NG–Fe_2	–3.35	2.08	0.195	0.184	–	–
NG–Cr_2	–2.68	2.40	0.158	0.155	–	–
NG–Cu_2	–2.61	2.12	0.076	–0.083	–	–
NG–Pb_2	–1.28	3.80	0.035	0.035	–	–
NG–Zn_2	–1.13	3.62	0.012	0.012	–	–
NG–Fe_3	–3.70	2.08	0.200	0.201	0.203	–
NG–Cr_3	–3.27	2.36	0.131	0.231	0.203	–
NG–Cu_3	–2.83	2.14	0.182	0.181	0.047	–
NG–Pb_3	–1.32	3.98	0.014	0.015	0.019	–
NG–Zn_3	–1.09	3.60	0.008	0.009	0.009	–
NG–Fe_4	–3.91	2.03	0.179	0.228	0.231	0.027
NG–Cu_4	–3.50	2.11	0.174	–0.094	–0.092	0.099
NG–Cr_4	–3.13	2.22	0.078	0.159	0.209	0.134
NG–Pb_4	–2.52	4.59	0.075	–0.060	–0.015	0.059
NG–Zn_4	–1.45	3.70	0.008	0.011	0.014	–0.010

and NG, and Mulliken charges for each atom of the corresponding systems were reported.

From the information shown above, the following tendencies were obtained: NG–Fe > NG–Cr > NG–Cu > NG–Pb>NG–Zn for n=2 and 3, and NG–Fe>NG–Cu>NG–Cr> NG–Pb > NG–Zn, for n = 4, respectively. It is inferred that these share some peculiar features such as Fe, Pb, and Zn being in the first, fourth, and last place in E_{ads} for all cases (n = 2, 3, and 4). These tendencies nearly agree with Fig. 3(A) of the experimental part, and the discontinuities can be associated to the different functional groups (Table 2) that remain on the AC after the combustion of each raw material (agave, broccoli, etc.). The adsorption effect will be explained by means of Mulliken charge analysis to evaluate the amount of electron transfer between the metallic clusters and the NG. From Table 3, the Fe_2 dimer shows the best electronic transfer towards the surface of the carbon compared with the Zn_2 dimer, where this effect is negligible. Therefore, iron presented the best adsorption, and zinc had the worst. This tendency remains for trimers and tetrahedrons of these two metals. However, the exception was copper (n = 2, 3, and 4), which changes from third (dimmer and trimer) to second place for tetrahedron geometries, respectively. Cu_2, Cu_3, and Cu_4 clusters prefer the top site of adsorption. Also, for four atoms, the initial configuration was a regular tetrahedron, but the final structure was a regular rhombus with an atom attached to its surface. This can be appreciated in Fig. 1(E). For the Pb_4 cluster, a similar behavior was found (Fig. 1(F)). However, this geometry was found parallel to the surface. For the rest of the clusters considered (Fe_4, Cr_4, and Zn_4), they displayed the form of tetrahedrons with a slight distortion on their structure, and for this disposition, the best adsorption is shown in Table 3. On the other hand, the whole set of metallic clusters was set preferably in horizontal way over the surface of carbon, with the exception of Cu_n where n = 2, 3, and 4 as it has been mentioned. The isosurfaces of electronic density for iron and zinc are shown in Fig. 2 to compare the best and worst cases. This way, the differences between them can be appreciated. For the systems that have the best adsorption properties (Fe_2, Fe_3, and Fe_4), the electronic charge is concentrated on the dimer (perpendicular or parallel), tetrahedron or rhombus, depending on the case; however, in the worst cases (Zn_2, Zn_3, and Zn_4), in the bonding zone between the cluster and NG, a "meniscus" that means weak electronic transfer is visible. Therefore, the adsorption is less compared with the other systems. Despite this discussion, all the systems analyzed exhibit high adsorption capabilities. Their values range between –1.09 and –3.91 eV. Hence, chemisorption effect is generated in all of them. Furthermore, it was found that short bond distances between the cluster and the surface of the carbon generate better values of adsorption energy than the longer ones (Table 3). This occurs because electronic density can migrate or be shared at smaller distance, regardless if the position of the cluster is on top or parallel to the NG. However, the values of bond distances for Pb_n are slightly larger than those corresponding to Zn_n (n = 2 and 4) systems, but in adsorption, this situation changes. This occurs because Pb is found in the carbon "family", so they share the same electronic configuration, whereas Zn has a closed electronic shell. Also, Pb possesses more electronegativity than Zn: 2.33 and 1.65, respectively.

4. Conclusions

The LA and the AC prepared from vegetable residues proved effective in removing heavy metals. The best inexpensive LA, prepared without combustion of the solid wastes, were BrocNat and Tuna when all five metals were mixed. They removed 3.3 mg of heavy metals per gram of vegetable residues. The best carbon, prepared from an abundant solid waste avoiding the using of wood during its preparation, was CarAgaQ. Using this carbon, it was possible to remove up to 6.7 mg/g of Pb (97%). Besides, it was able to remove 9.98 mg/g of a mixture of five heavy metals at pH = 1.

When the pH was slightly increased, the adsorption capacity of all the AC was improved significantly. At pH = 2, CarAgaQ was able to adsorb 19.55 mg/g of the five heavy metals.

DFT calculations were carried out to establish the tendency of adsorption energy of metallic clusters on a carbon surface, this was simulated as an NG. The values on adsorption for Fe, Pb, and Zn were invariants for the sizes analyzed in this study. The iron showed the best bond to the surface, whereas Zn was the case with less preference, however, a clearly tendency was obtained at least for the first stages of adsorption for this metals.

Acknowledgments

A.A. Peláez-Cid would like to thank PRODEP for the economic support during her research stay at UAEH (Grant number: 14/9726) and BUAP-CA-236. The authors would like to thank H. Welti-Peláez for his assistance in the English language.

Symbols

LA	—	Lignocellulosic adsorbents
AC	—	Activated carbons
Tuna	—	Prickly pear peel adsorbent
BrocNat	—	Broccoli stem adsorbent
EmbZap	—	White sapote seed adsorbent
FAgaNat	—	Agave fiber adsorbent
CarTunaQ	—	Prickly pear peel carbon
CarBrocQ	—	Broccoli stem carbon
CarZapQ	—	White sapote seed carbon
CarAgaQ	—	Agave fiber carbon
DFT	—	Density functional theory
NG	—	Nanosheet of graphene
S_{BET}	—	Specific surface area

References

[1] E.A. Deliyanni, G.Z. Kyzas, K.S. Triantafyllidis, K.A. Matis, Activated carbons for the removal of heavy metal ions: a systematic review of recent literature focused on lead and arsenic ions, Open Chem., 13 (2015) 699–708.
[2] M. Kazemipour, M. Ansari, S. Tajrobehkar, M. Majdzadeh, H.R. Kermani, Removal of lead, cadmium, zinc, and copper from industrial wastewater by carbon developed from walnut, hazelnut, almond, pistachio shell, and apricot stone, J. Hazard. Mater., 150 (2008) 322–327.
[3] L. Mouni, D. Merabet, A. Bouzaza, L. Belkhiri, Adsorption of Pb(II) from aqueous solutions using activated carbon developed from apricot stone, Desalination, 276 (2011) 148–153.
[4] M. Kobya, E. Demirbas, E. Senturk, M. Ince, Adsorption of heavy metal ions from aqueous solutions by activated carbon prepared from apricot stone, Bioresour. Technol., 96 (2005) 1518–1521.
[5] L. Semerjian, Equilibrium and kinetics of cadmium adsorption from aqueous solutions using untreated *Pinus halepensis* sawdust, J. Hazard. Mater., 173 (2010) 236–242.
[6] F. Fu, Q. Wang, Removal of heavy metal ions from wastewaters: a review, J. Environ. Manage., 92 (2011) 407–418.
[7] I.A. Aguayo-Villarreal, A. Bonilla-Petriciolet, V. Hernández-Montoya, M.A. Montes-Morán, H.E. Reynel-Avila, Batch and column studies of Zn^{2+} removal from aqueous solution using chicken feathers as sorbents, Chem. Eng. J., 167 (2011) 67–76.
[8] M.A. Hashim, S. Mukhopadhyay, J.N. Sahu, B. Sengupta, Remediation technologies for heavy metal contaminated groundwater, J. Environ. Manage., 92 (2011) 2355–2388.
[9] T.A. Kurniawan, G.Y.S. Chan, W.H. Lo, S. Babel, Physico–chemical treatment techniques for wastewater laden with heavy metals, Chem. Eng. J., 118 (2006) 83–98.
[10] H.A. Hegazi, Removal of heavy metals from wastewater using agricultural and industrial wastes as adsorbents, HBRC J., 9 (2013) 276–282.
[11] A. Ahmad, M. Rafatullah, O. Sulaiman, M.H. Ibrahim, Y.Y. Chii, B.M. Siddique, Removal of Cu(II) and Pb(II) ions from aqueous solutions by adsorption on sawdust of Meranti wood, Desalination, 247 (2009) 636–646.
[12] F. Boudrahem, F. Aissani-Benissad, H. Aït-Amar, Batch sorption dynamics and equilibrium for the removal of lead ions from aqueous phase using activated carbon developed from coffee residue activated with zinc chloride, J. Environ. Manage., 90 (2009) 3031–3039.
[13] G.Z. Kyzas, E.A. Deliyanni, K.A. Matis, Activated carbons produced by pyrolysis of waste potato peels: cobalt ions removal by adsorption, Colloids Surf., A, 490 (2016) 74–83.
[14] A.A. Peláez-Cid, I. Velázquez-Ugalde, A.M. Herrera-González, J. García-Serrano, Textile dyes removal from aqueous solution using *Opuntia ficus-indica* fruit waste as adsorbent and its characterization, J. Environ. Manage., 130 (2013) 90–97.
[15] A.A. Peláez-Cid, A. Vázquez-Barranco, A.M. Herrera-González, Elimination of dyes present in textile industry wastewater using adsorbent materials prepared from broccoli stem, Adv. Mater. Res., 976 (2014) 207–211.
[16] A.A. Peláez-Cid, A.M. Herrera-González, A. Bautista-Hernández, M. Salazar-Villanueva, Preparation and characterization of activated carbon from *Agave tequilana* Weber for the removal of textile dyes and heavy metals, Desal. Wat. Treat., 57 (2016) 21105–21117.
[17] A.A. Peláez-Cid, M.A. Tlalpa-Galán, A.M. Herrera-González, Carbonaceous material production from vegetable residue and their use in the removal of textile dyes present in wastewater, Mater. Sci. Eng., A, 45 (2013). doi:10.1088/1757-899X/45/1/012023.
[18] A.A. Peláez-Cid, A.M. Herrera-González, M. Salazar-Villanueva, A. Bautista-Hernández, Elimination of textile dyes using activated carbons prepared from vegetable residues and their characterization, J. Environ. Manage., 181 (2016) 269–278.
[19] C.J. Durán-Valle, Geometrical relationship between elemental composition and molecular size in carbonaceous materials, Appl. Surf. Sci., 252 (2006) 6097–6101.
[20] K.E. Schriver, J.L. Persson, E.C. Honea, R.L. Whetten, Electronic shell structure of group-IIIA metal atomic clusters, Phys. Rev. Lett., 64 (1990) 2539–2542.
[21] D.E. Bergeron, A.W. Castleman, T. Morisato, S.N. Khanna, Formation and properties of halogenated aluminum clusters, J. Chem. Phys., 121 (2004) 10456–10466.
[22] R. Gaudoin, W.M.C. Foulkes, Ab initio calculations of bulk moduli and comparison with experiment, Phys. Rev. B, 66 (2002) 1–4.
[23] S.H. Yang, D.A. Drabold, J.B. Adams, A. Sachdev, First-principles local-orbital density-functional study of Al clusters, Phys. Rev. B, 47 (1993) 1567–1576.